Editors' Suggestion

Novel dipole-lattice coupling in the quantum spin liquid material κ-(BEDT-TTF)$_2$Cu$_2$(CN)$_3$

Jesse Liebman,[1] Kazuya Miyagawa,[2] Kazushi Kanoda,[2] and Natalia Drichko[1,*]
[1]*Department of Physics and Astronomy, The Johns Hopkins University, Baltimore, Maryland 21218, USA*
[2]*Department of Applied Physics, University of Tokyo, Tokyo 113-8656, Japan*

(Received 26 March 2024; revised 21 August 2024; accepted 4 September 2024; published 2 October 2024)

A family of molecular Mott insulators on triangular lattice has provided a few $S = 1/2$ triangular quantum spin liquid candidates, with κ-(BEDT-TTF)$_2$Cu$_2$(CN)$_3$ being the most studied material of this group. The large number of experimental works present a conflicting set of evidence, with some suggesting spin liquid behavior, while others pointing towards a valence bond solid with orphan spins. In this work we use Raman scattering spectroscopy to probe both local charge on molecular sites and lattice phonons as a function of temperature down to 6 K. Based on the analysis of the line shape of the BEDT-TTF charge sensitive vibration ν_2 on cooling below 40 K, we suggest the development of disordered fluctuating charge disproportionation on (BEDT-TTF)$_2$ dimers of amplitude as small as $0.05e$. The lattice phonons show strong anomalous broadening on cooling only in the (c,c) scattering channel, associated with the developing charge disproportionation. We suggest an interpretation, where the coupling of disordered charge dipoles on dimers to the lattice results in anisotropic modulation of charge transfer integrals between dimer lattice sites. Such fluctuations would result in modulation of magnetic coupling between spins which can produce fluctuating charge ordered spin-singlet pairs.

DOI: 10.1103/PhysRevB.110.165105

I. INTRODUCTION

In strongly correlated systems, exotic physics and critical behavior emerge at the junction of geometric frustration and competing interactions. One example is the quantum spin liquid (QSL), where emergent fractional spin excitations arise from an infinitely degenerate collective electronic quantum state. Ever since Anderson suggested a resonating valence bond (RVB) ground state [1], Mott insulators with spin $S = 1/2$ on a triangular lattice and nearest-neighbor anitferromagnetic interactions have been studied in order to realize the QSL. However, further studies have shown that realization of the QSL requires interactions beyond nearest neighbors [2–4]. Additionally, molecular spin liquid candidates, one of which we discuss in the present work, were suggested as providing an alternative way to realize the QSL state. Fluctuating electric dipoles which form on molecular dimer sites due to Coulomb interactions and are coupled to spins, preventing magnetic order, were suggested as a way to stabilize the QSL [5]. The discussion of whether charge and spin degrees of freedom would compete or interact, resulting in a new type of spin liquid, is still ongoing.

Molecular Mott insulators with the so-called κ-phase structure realize a $S = 1/2$ antiferromagnet on a triangular lattice. In these layered molecular materials, the lattice of the functional layer is formed by pairs of BEDT-TTF molecules [6] (referred to as ET) that share one hole ($+1e$). The $(ET)_2^{1+}$ dimer units carry spin $S = 1/2$ and form a triangular crystal layer, where overlapping π orbitals of ET molecules result in electronic bands. The electronic overlap between nearest dimers is parametrized by the charge transfer integral t and the on-site electron repulsion is parametrized through the double-occupancy energy U. The large ratio of U/t results in a Mott insulator state for some of these materials, with antiferromagnetic interactions between $S = 1/2$ spins. Two possible scenarios are proposed for these materials to realize a QSL state; one is a ring exchange preventing 120 degree order [3,7]. Another is an exotic "quantum dipole liquid" [5], where spins are coupled to the fluctuating electric dipoles formed on $(ET)_2^{1+}$ dimers as a result of electronic correlations (see Fig. 1 for the illustration of the charge degree of freedom). The quantum dipole liquid, first suggested in connection with the nontrivial dielectric behavior of κ-(ET)$_2$Cu$_2$(CN)$_3$ [8–10], was observed in another molecular Mott insulator [11]. Coupling of charge and spin degrees of freedom in these organic Mott insulators demonstrate a unique multiferroic behavior. While other multiferroic materials exist with competing interactions, most have distinct sublattices for ferroelectricity and magnetism. The κ-(ET)$_2$X materials are special as the charge and spin degrees of freedom belong to one correlated electron system.

κ-(ET)$_2$Cu$_2$(CN)$_3$ (κ-Cu-CN) is the most thoroughly studied of these materials. Antiferromagnetic interactions J between $S = 1/2$ on the $(ET)_2^{1+}$ was shown to be on the order of 200 K [12]. The QSL ground state of this material was suggested based on the absence of magnetic ordering down to $T = 32$ mK [12], despite large AF interactions. The robustness of a description by $S = 1/2$ magnetism on a triangular lattice with J of about 200 K was confirmed by observation of spin excitations in Raman scattering [11,13]. A linear contribution to the specific heat insensitive to magnetic field was attributed to gapless fermionic excitations [14].

*Contact author: drichko@jhu.edu

 ©2024 American Physical Society

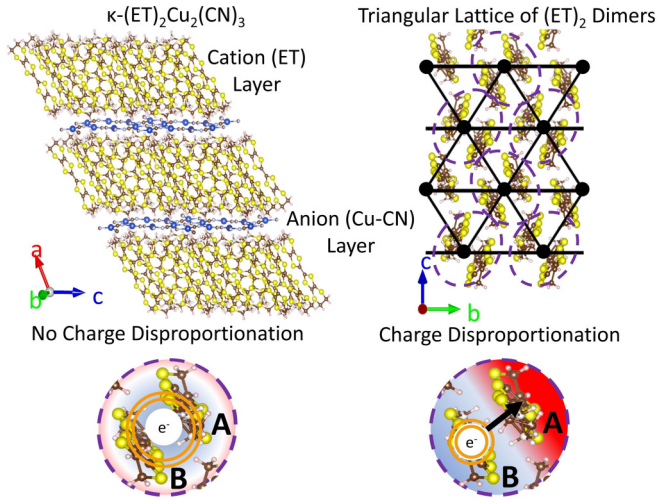

FIG. 1. Structure of κ-$(ET)_2Cu_2(CN)_3$. ET layers are separated by Cu-CN layers. ET molecules form dimers on a triangular lattice. Within an $(ET)_2^{1+}$ dimer, the HOMO electron can be shared equally (no charge disproportionation, left panel) or unequally (charge disproportionation, lower right panel) with the resulting electric dipole vector shown as a black arrow.

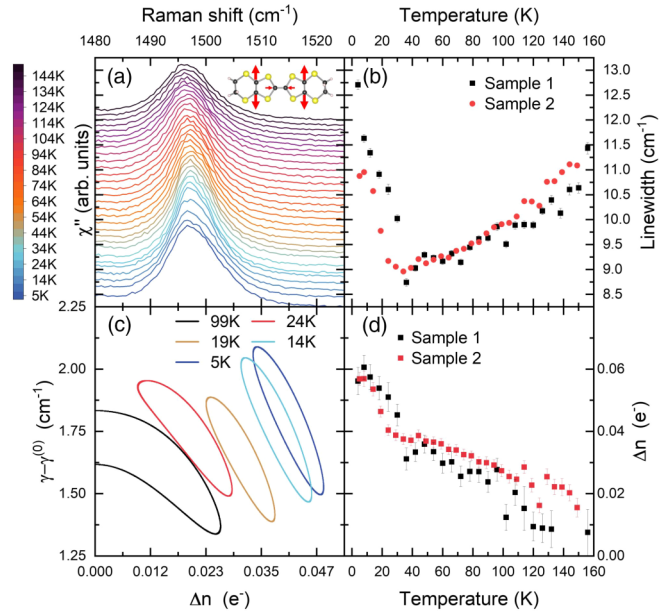

FIG. 2. (a) Raman scattering spectra of κ-$(ET)_2Cu_2(CN)_3$ in the frequency region of molecular vibration ν_2 in the (b,c) scattering channel, sample 2. Spectra are shifted along the y axis for clarity. (b) The temperature dependence of the linewidth (FWHM) of ν_2 molecular vibration. (c) Boundaries of 1σ confidence regions for fit parameters of the charge glass model for sample 2: charge disproportionation Δn and Lorentzian width parameter $\gamma - \gamma^{(0)} \propto \omega_{\text{decay}}^{-1}$, where ω_{decay} is charge fluctuation frequency. Note the narrowing of the parameters region and the increase of Δn with temperature decrease. (d) Temperature dependence of the charge disproportionation Δn obtained from the fit of the ν_2 line shape with the case of the static charge glass model.

The QSL nature of κ-Cu-CN has been actively discussed recently, starting with the thermal transport [15] measurements. The nuclear magnetic resonance (NMR) [16] and electron spin resonance (ESR) [17] measurements indicate a low-temperature decrease in spin susceptibility reminiscent of spin-singlet formation with a finite residual susceptibility, which was argued to come from orphan spins [17–19]. An anomalous lattice response and entropy release are observed at 6 K without a clear phase transition [20]. Multiple spectroscopic studies of κ-Cu-CN material [10,21–24] point towards possible unconventional behavior of the charge degree of freedom and the lattice, but have not produced conclusive results.

Presented in this work are Raman scattering measurements of κ-Cu-CN conducted in a broad frequency range from 12 up to 2000 cm^{-1} down to 6 K, which allows us to uncover glassy (disordered) charge fluctuations within $(ET)_2^{1+}$ dimers and the interaction of these charge fluctuations with the lattice. The quantitative analysis of the line shapes of lattice phonons and molecular vibrations allows us to follow the temperature dependence of the frequency of charge fluctuations. Our observations are consistent with the emergence of an electric dipole glass state in κ-Cu-CN. We speculate that the dipole glass state corresponds to disorder in the magnetic exchange constant J, which promotes spin-singlet formation and a valence bond glass state.

II. RESULTS

A. Fluctuating charges probed by molecular vibrations

As the first step, we reexamine the line shape of a vibration of the central C=C bond of ET molecules ν_2, which is an accepted tool to study the distribution of the charge in the highest occupied molecular orbital (HOMO) of an ET molecule. For a detailed explanation of the line shape analysis and fitting procedure, see the Supplemental Material [25]. The frequency of ν_2 (in cm^{-1}) satisfies the relation

$$\omega(n) = 1447\ \text{cm}^{-1} + 120(1e^- - n)\frac{\text{cm}^{-1}}{e^-}, \qquad (1)$$

where n is the average charge on the ET molecule, with $n = 0.5e^-$ in most ET-based materials [26]. As demonstrated in Fig. 2(b) by the temperature dependence of the full width at half maximum (FWHM), we observe that ν_2 narrows on cooling down to approximately 40 K, but broadens on cooling below this temperature. In Fig. 2 we plot results obtained for two samples, which show a similar behavior with temperature with small discrepancies. ν_2 frequency does not show any anomaly or splitting upon cooling, in agreement with the previous studies [10].

In our analysis of the line shape of ν_2, we considered two possible scenarios.

(i) Static or fluctuating charge order between sites A and B. Charge order is defined by a charge separation, $\Delta n = n_A - n_B$, which results in a frequency splitting, $\Delta\omega_{AB}$. Charge disproportionation within an $(ET)_2^{1+}$ dimer creates an electric dipole, as shown in Fig. 1. We assume that in a static regime each component possesses a similar lifetime as the nonperturbed ν_3 vibration, which provides a "natural" linewidth (in our case, 5 cm^{-1}). A frequency of fluctuations, ω_{ex}, is defined as the hopping rate between sites [11,27–29]. Static

charge order is the case with $\omega_{ex} = 0$. The static and dynamic cases result in a renormalized Lorentzian line shape of the response.

(ii) Disordered charge model. A Gaussian parameter describes a random distribution of charge as charge fluctuations with a stochastic decay process. It is modeled by the autocorrelation function of charge fluctuations

$$\Delta_n^2(\tau) \equiv \langle \Delta n(\tau)\Delta n(0)\rangle = \Delta_n^2 \exp(-\omega_{\text{decay}}\tau), \quad (2)$$

where Δ_n is the amplitude of charge fluctuations and ω_{decay} is the inverse lifetime of charge fluctuations [27–29]. In the dimerized κ phase we expect that the total charge on the dimer $(\text{ET})_2^{+1}$ is constant $n = +1e$. Therefore, for the molecules A and B within each dimer, $n_A + n_B = +1e$, which imposes the limit of the fit parameter $\Delta n = |n_A - n_B|$. The resulting line shape is a renormalized Voigt profile, characterized by a Lorentzian width γ that is determined by the decay frequency of charge fluctuations ω_{decay}

$$\gamma = \gamma_0 + C^2 \frac{\Delta\omega^2}{\omega_{\text{decay}}} \quad (3)$$

and Gaussian variance

$$\sigma^2 = \sigma_{\text{res}}^2 + \Delta\omega^2, \quad (4)$$

where γ_0 is the natural lifetime of the pure vibration, C is a constant, $\Delta\omega = \frac{120\ \text{cm}^{-1}}{e^-}\Delta_n$, and σ_{res} is the spectral resolution. In a static case where the dynamic process freezes entirely, the Gaussian variance of frequency $\Delta\omega^2$ will define the line shape.

For the case of relatively weak broadening of ν_2, the analysis of the experimental spectra with both models has the following limitation: we cannot uniquely determine the charge separation and fluctuation rate, which may be both temperature dependent, and have large covariance. The increase of charge separation leads to an increase of the linewidth [Lorenzian for model (i) and Gaussian for model (ii)], while the increase of fluctuation frequency leads to a decrease of the Lorentzian linewidth.

A static case of both models provides a limit on the estimate of the charge separation. A fit with the static charge order [model (i)] yields $\Delta n = 0.05e$ at the lowest measured temperature of 6 K, which is shown in the Supplemental Material [25]. Introducing fluctuations in model (i) increases charge separation, so the static case provides a lower limit for charge separation in model (i). The static case ($\omega_{\text{decay}} \to 0$) of the disordered charge distribution [model (ii)] yields a standard deviation of charge of $0.03e$ and an average charge separation of $0.06e$ in a dimer. Introducing fluctuations in model (ii) decreases the average charge separation to $0.05e$; therefore, the static case provides an upper bound for average charge separation. Figure 2(d) shows the temperature dependence of the average charge separation for a static case. However, the static case provides worse fit quality than dynamic charge disproportionation.

To identify the best fit parameters we used the total squared error as a measure of goodness of fit (see the Supplemental Material [25]), which is calculated as $TSE_{\text{model}} = \sum_{i=1}^{N}[I(\omega)_{\text{meas}} - I(\omega)_{\text{model}}]^2$. While the error is quantitatively different for the two measured samples, the final result is that the best fit is provided by the Gaussian shape (disordered charge model). The values of Δn and ω_{decay} suggested by 95% fit confidence regions [30] are shown in Fig. 2(c). The range of parameters narrows on cooling, which conclusively shows that charge disproportionation increases. The best fit provides a broad range for fluctuation frequencies that is larger than the variation of frequency with temperature, as shown by the 95% confidence regions at a few different temperatures [see Fig. 2(c)].

The main result of this analysis is that the charge disproportionation abruptly increases below 40 K, begins to flatten near 20 K, and remains flat below 10 K, in agreement with the results of Refs. [22,26]. We find that this charge disproportionation is disordered and slowly fluctuating. Vibrational analysis cannot follow the frequency of fluctuations precisely. The average charge separation at the lowest temperatures measured about 6 K is estimated to be $0.05e$, which is very close to the estimate provided by dielectric measurements in Ref. [8]. This is significantly smaller than the charge separation observed in κ-$(\text{ET})_2\text{Hg}(\text{SCN})_2\text{Cl}$, the only material with a static charge ordered state [31,32].

B. Lattice response

Next, we examine the lattice response of κ-Cu-CN by analyzing the Raman scattering spectra in the (b,b), (b,c), and (c,c) scattering channels at low frequencies. Lattice phonons in ET-based compounds are typically observed in the frequency range below approximately 100 cm^{-1} [23]. In Fig. 3 we show the Raman spectra in the (b,b), (c,c), and (b,c) polarizations from 12.5 $\text{cm}^{-1}$to 112.5 cm^{-1}. The spectra in the higher frequency range are shown in Fig. 4. The assignment of the observed modes is based on calculations [23] that are presented in the Supplemental Material [25]. One has to keep in mind that these lattice modes are superimposed on the continuum of the magnetic excitations, which is about an order of magnitude weaker than the observed phonons and detected in low resolution broad range measurements [13,33].

The lattice modes in this spectral region are overdamped and weak at room temperature, but can be distinctly observed at temperatures below approximately 150 K. The changes of phonons on cooling in the (b,b) and (b,c) channels are conventional: the phonons harden and narrow on cooling, their width described by anharmonic decay according to the Klemens model [34] [see Fig. 5(a)]. All of these modes increase in intensity on cooling. In the (b,c) channel we observe an appearance of the mode A at 38 cm^{-1} below approximately 20 K.

In the (c,c) scattering channel, we observe conventional behavior of the width and frequencies of the lattice modes only down to approximately 20 K. Below 20 K the modes labeled A–H broaden and lose coherent spectral weight, with the strongest effect observed for the mode B at 46 cm^{-1} [Fig. 3(c)]. The linewidth increases on cooling below 20 K down to 6 K [Fig. 5(b)]. Several of the modes, notably B, C, and D, become so broad and incoherent below 10 K that one cannot isolate their line shape. The fit parameters are therefore not definitive, but represent a best fit with appropriate uncertainties.

All of the modes A–H correspond to the motion of ET molecules [23]. For some there is coupled anion motion, but the mode F corresponds to purely ET motion.

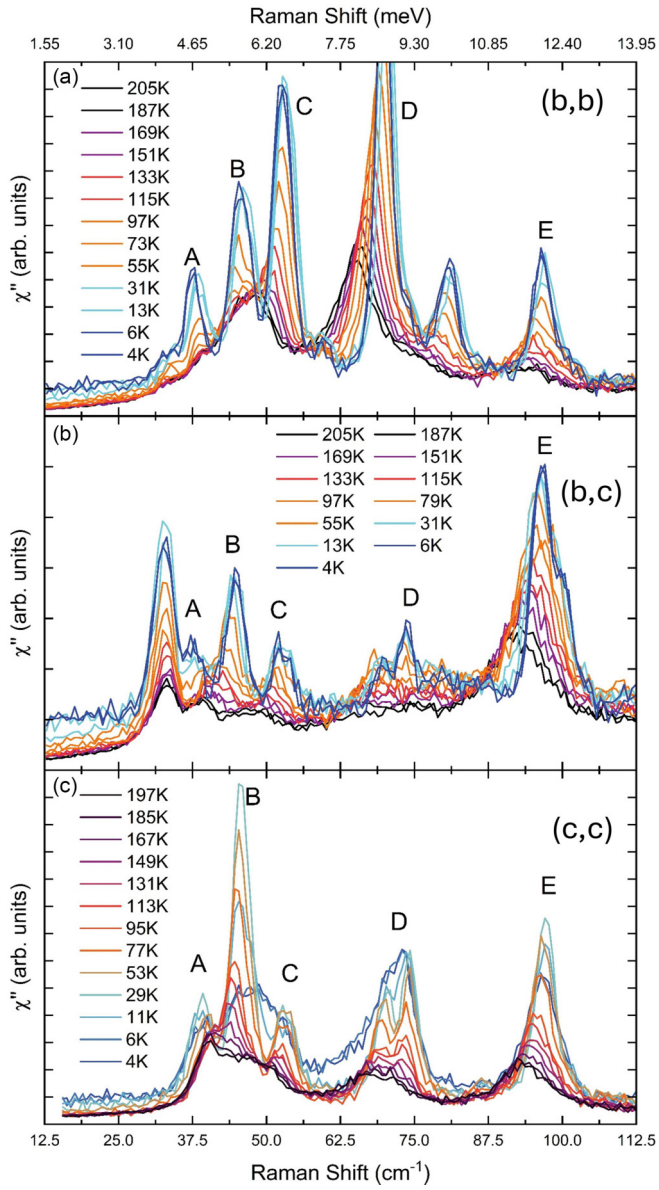

FIG. 3. Temperature dependence of the Raman scattering spectra of κ-$(ET)_2Cu_2(CN)_3$ in the spectral range where lattice phonons are observed (below 110 cm^{-1}) in the (a) (b,b), (b) (b,c), and (c) (c,c) scattering channels.

The anisotropy of the broadening of phonons at low temperatures, which is observed only in the (c,c) polarization, is the most striking result. We do not observe recovery of the width of the phonons down to the lowest measured temperature of 6 K, while neutron scattering results, though measured with lower energy resolution, suggested such a drop below 6 K [24].

III. DISCUSSION

A. Development of glassy charge disproportionation

The local probe of charge on ET molecules, provided by the analysis of the line shape of the molecular vibration ν_2, reveals the following picture. Below 40–60 K, the local probe signals an increasing amplitude of charge fluctuations. Both the onset temperature of charge separation of 60 K and its

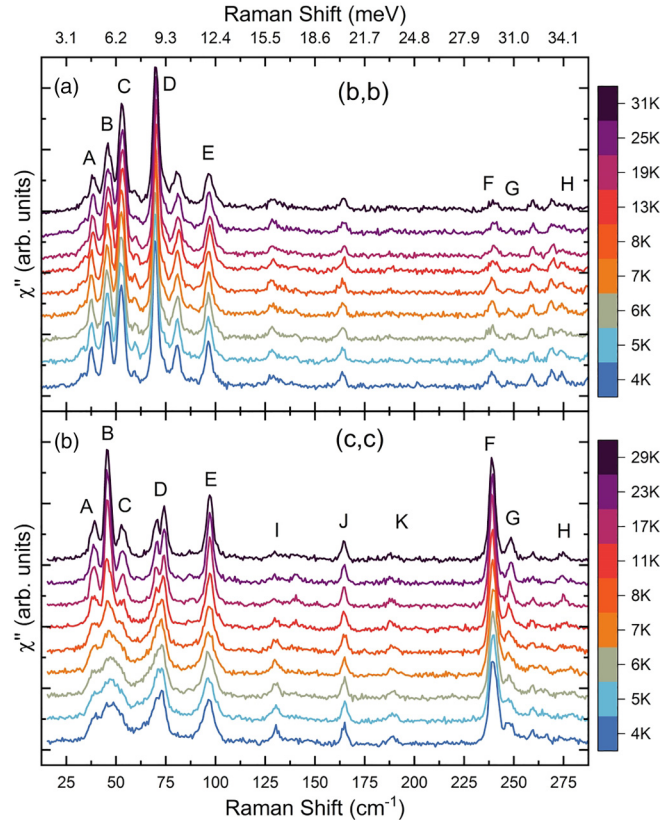

FIG. 4. Temperature dependence of the Raman scattering spectra of κ-$(ET)_2Cu_2(CN)_3$ in the frequency range below 300 cm^{-1} below 31 K in (a) (b,b) and (b) (c,c) scattering channels. Spectra are offset for clarity. Phonons are marked A–H.

amplitude, estimated at $\Delta n = 0.03e$ at 60 K and increasing to $\Delta n = 0.05e$ at 6 K, observed by us are in agreement with the dielectric measurements [8,9] and the broadening of the charge sensitive mode ν_{27} observed by infrared spectroscopy [22].

On further cooling, we can identify two characteristic temperatures from the collective response provided by the analysis of the lattice phonons: At 20 K lattice modes in the (c,c) channel demonstrate broadening, which saturates at 6 K. This coincides with the appearance of the mode A at 38 cm^{-1} in the (b,c) channel, demonstrating the loss of local inversion symmetry. These temperature scales also correspond to those observed in the measurements of dielectric properties. Below 20 K, a freezing out of the high-temperature dielectric process with glassy relaxation is suggested [9], where the 6 K anomaly [20] could be a transition into a spin-singlet glassy state [17,18]. The Gaussian distribution of electric dipole moments and freezing out of fluctuations can serve an evidence for the glassy behavior of the observed charge disproportionation [35].

The anion layer was previously suggested as a source of the disorder potential [9,36], which can be a candidate for the origin of a glassy state. However, we cannot attribute the lattice phonons broadening to structural disorder: the increase in linewidth of the lattice modes is observed only in the (c,c) channel and only in the $(ET)_2^{1+}$ phonons, without broadening vibrations of the anion layer, such as the lattice

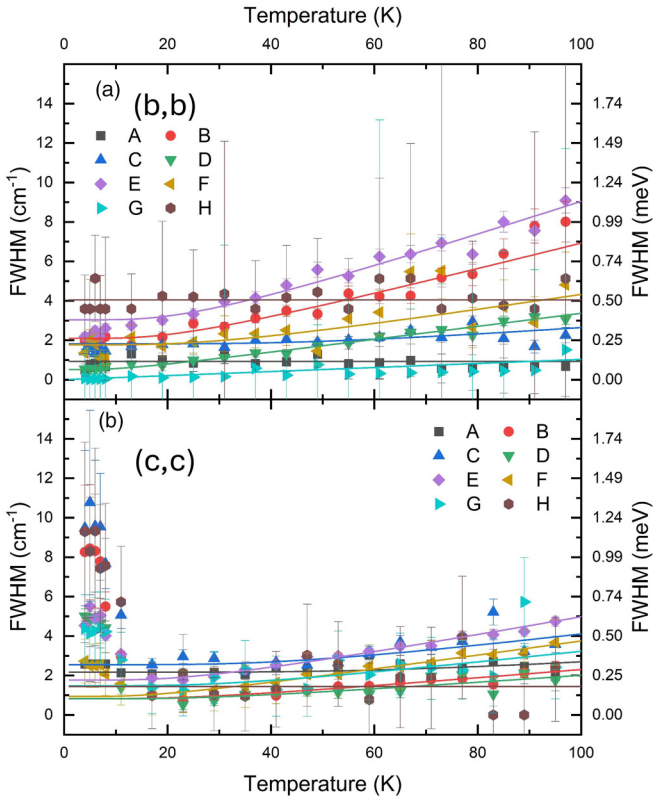

FIG. 5. Full width at half maximum of modes of lattice vibrations of κ-$(ET)_2Cu_2(CN)_3$ A–H (see notations in Fig. 4) in (a) (b,b) and (b) (c,c) polarizations. The solid lines are fits according to Ref. [34], where the fits are performed with data from temperatures above 30 K.

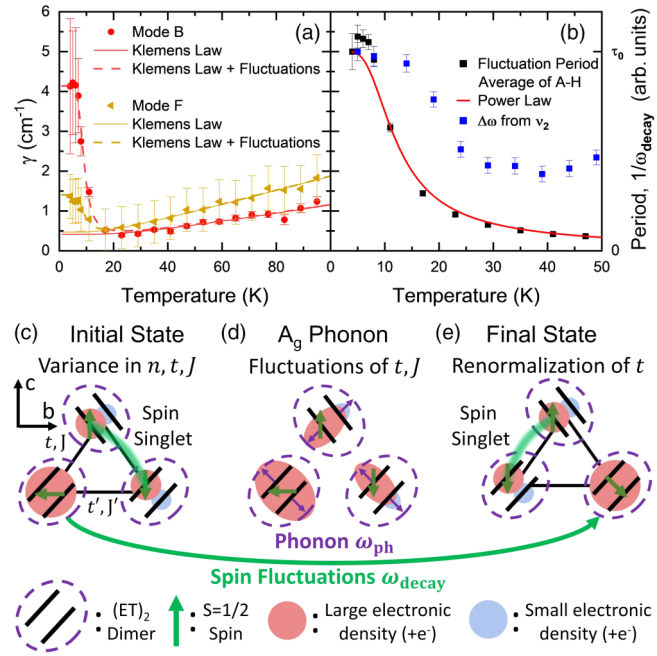

FIG. 6. Interaction of fluctuations and phonons. (a) The decay rate of modes B and F from data, conventional decay, and additional scattering from fluctuations. (b) Lifetime of charge fluctuations, estimated using Eq. (11). (c), (d), (e) Scattering of defects by phonons. (c) An initial state of the valence bond solid. (d) A Raman active phonon changing the charge transfer integrals. (e) A final state of the valence bond solid.

modes I, J, and K. An alternative way to obtain a fluctuating system with a broad range of spatial and temporal correlations was suggested by torque magnetometry in another ET-based Mott insulator, κ-$(ET)_2Hg(SCN)_2Br$, which is close to a ferroelectric phase transition [37]. In κ-$(ET)_2Hg(SCN)_2Br$ the intrinsic dynamic disorder is a consequence of competition between long range Coulomb repulsion and antiferromagnetic interactions between correlated $S = 1/2$ holes $(+e)$ [37]. Below we discuss the importance of electron-phonon coupling for the observed dynamic disorder and low temperature glassy state.

B. Modeling electron-phonon coupling

Theoretical understanding of charge order in ET-based dimer Mott insulators has been suggested either within an extended Hubbard model for 1/4 filled bands with electron-phonon coupling [38] or by mapping the charge degree of freedom within dimer lattice sites onto a $S = 1$ Ising model, coupled to $S = 1/2$ Heisenberg spin interactions in a Kugel-Khomskii model [5,39,40]. The basic parameters of the extended Hubbard model with each $ET^{+0.5}$ molecule counted as a lattice site are electron repulsion U, V, and charge transfer integrals t, where t_d is a charge transfer integral between the molecules within a $(ET)_2^{1+}$ dimer (see Fig. 6). The hybridization of the ET HOMO within $(ET)_2^{1+}$ dimers renormalizes the nearest neighbor repulsion within a dimer, V_d, to an effective on-site Coulombic interaction:

$$U_{\text{eff}} = 2t_d + V_d + \frac{U - V_d}{2}\left(1 - \sqrt{1 + \left(\frac{4t_d}{U - V_d}\right)^2}\right). \quad (5)$$

This allows a mapping of a 1/4-filled model onto a 1/2-filled model with the following Hamiltonian describing interactions between dimer lattice sites:

$$H_1 = U_{\text{eff}} \sum_{\text{sites } i} n_{i\uparrow} n_{i\downarrow} + \sum_{i \neq j} V_{ij}(n_{i\uparrow} + n_{i\downarrow})(n_{j\uparrow} + n_{j\downarrow}) - \sum_{i \neq j} \sum_{\text{spin } \sigma} t_{ij}(c^{\dagger}_{i\sigma} c_{j\sigma} + \text{H.c.}), \quad (6)$$

where (next) nearest neighboring lattice sites have Coulombic repulsion $(V')\ V$ and charge transfer integrals $(t')\ t$. The spin interactions are described by magnetic exchange parameters $J = \frac{4t^2}{U_{\text{eff}}}$ and $J' = \frac{4t'^2}{U_{\text{eff}}}$ [5]. The dimer Mott insulator to charge order insulator transition has been parametrized via competition between intramolecular hopping (t_d) and interdimer Coulomb repulsion (V) [5,38,39] and the anisotropy of interdimer hopping (t'/t) [38]. In κ-Cu-CN, t'/t is slightly above 0.8 [41–44], where geometric frustration is already large enough to avoid anisotropy-induced charge order, according to numerical simulations [38]. The most basic tuning of the dipole liquid to dipole solid transition is provided by the increase of $V/t_d, V'/t_d$ parameters [5,39]. In the dipole solid phase (static charge order) t, t' and V, V' are renormalized

due to unequal occupation within $(ET)_2^{1+}$ dimers, resulting in electronic anisotropy [45].

To the best of our knowledge, theoretical considerations have not accounted for *dynamic* renormalization of transfer integrals by charge fluctuations in a dipole liquid state. We expect that this modulation of transfer integrals would result in electron-phonon coupling to the lattice phonons. Lattice phonons A–H modulate the distance between the planes of ET molecules, the angle between ET molecules, and the relative orientation of ethylene endgroups. Dynamic changes to these structural parameters with modulation of charge transfer integrals [46] is the microscopic mechanism of this electron-phonon coupling.

The emerging charge disproportionation occurs within $(ET)_2^{1+}$ dimers, so at this point we do not consider fluctuations in the amplitude of t_d. Charge fluctuations dynamically renormalize the charge transfer integral t [45], thus resulting in corresponding fluctuations of t:

$$\langle \delta t(\tau)\delta t(0)\rangle = \Delta_t^2 \exp(-\omega_{\text{decay}}\tau), \tag{7}$$

where $\Delta_t^2 = \langle(\bar{t} - t)^2\rangle$ and $\bar{t}$ is the average of t, and ω_{decay} is the average decay rate of charge fluctuations.

In a limit where fluctuation frequency is small, $\omega_{\text{decay}} < \omega_{\text{ph}}$, we can express phonon frequency ω_{ph} as a function of the change of transfer integral δt:

$$\omega_{\text{ph}}(\delta t) = \omega_{\text{ph}}^{(0)} + \delta t \frac{\partial \omega_{\text{ph}}}{\partial t} + O(\delta t^2), \tag{8}$$

where $\omega_{\text{ph}}^{(0)}$ is a lattice phonon frequency at the average value of t or $\delta t = 0$. $\frac{\delta\omega_{\text{ph}}}{\delta t}$ is a strength of electron-phonon coupling which can be different for every lattice mode. Such coupling will result in $\Delta\omega_i$, a deviation in frequency, arising from Δ_t, the amplitude of charge transfer integral fluctuations, so that $\Delta\omega_i^2 = \langle(\omega_i^{(0)} - \omega_i)^2\rangle = (\frac{\partial\omega_i}{\partial t}\Delta_t)^2$.

The linewidth of the lattice vibrations can then be expressed as

$$\gamma_i = \gamma_i^{(0)} + C_i^2 \frac{\Delta\omega_i^2}{\omega_{\text{decay}}}, \tag{9}$$

where $\gamma_i^{(0)}$ is the "natural" linewidth unperturbed by the charge fluctuations [34] and C_i is a constant different for every lattice mode. The line shape of the lattice vibrations A–H in the (c,c) scattering channel is Lorentzian, rather than Gaussian, below 20 K at least down to 6 K. This suggests that the broadening, or decreased lifetime, of the lattice modes is primarily determined by the decrease of ω_{decay}, or slowing of charge fluctuations, rather than an increase in structural disorder, or $\Delta\omega_i$. This is in contrast to the ν_2 mode, which is very sensitive to the redistribution of charges on the ET molecule and subsequent renormalization of t, meaning there is a large $\frac{\delta\omega_{\text{ph}}}{\delta t}$ and a Gaussian line shape.

Figure 6(a) shows the temperature dependence of the linewidth γ of two lattice modes, B and F, in the (c,c) scattering channel. At higher temperatures the modes narrow on cooling, following the Klemens model, while the broadening below 20 K is determined by the increased scattering by charge fluctuations.

For each mode, a deviation from the Klemens' law due to the enhancement of the phonon scattering rate is

$$\gamma_i' = \gamma_i - \gamma_i^{(0)} = C_i^2 \frac{\Delta\omega_i^2}{\omega_{\text{decay}}} = C_i^2 \Delta\omega_i^2 \tau_{\text{decay}}. \tag{10}$$

In order to determine the fluctuation lifetime τ_{decay} independently of C_i and $\Delta\omega_i$ which we assume to be temperature independent for the modes A–H, we can estimate

$$\tau_{\text{decay}}(T) = \frac{1}{N}\sum_{i=1}^{N} \frac{\gamma_i'(T)}{\gamma_i'(6\text{ K})}. \tag{11}$$

Such averaging provides a reliable result for the temperature dependence of τ_{decay}. Figure 6(b) demonstrates that the fluctuation lifetime increases as temperature decreases and reaches saturation as temperature approaches 6 K.

Since the magnetic exchange is $J = \frac{4t^2}{U_{\text{eff}}}$, we expect that fluctuations of t, Δ_t, correspond to fluctuations of J, $\Delta_J = \frac{8t}{U_{\text{eff}}}\Delta_t$. These fluctuations, which have a broad range of low frequencies below 6 K, can explain the origin of the disordered magnetic ground state and spin singlet pairs with lifetime of τ_{decay}, as measured in ESR [17], NMR, and torque magnetometry [18,47], and are consistent with a valence bond solid.

In Figs. 6(c)–6(e) we suggest a scheme for the microscopic origin of the coupling of the charge, spin, and lattice degrees of freedom. $(ET)_2^{1+}$ dimers are depicted by dashed circles which contain two ET molecules which are depicted by black lines. The charge density of the HOMO is depicted by red circles. In the initial state [snapshot 6(c)] we have two types of charge distribution on $(ET)_2^{1+}$ dimers: one dimer has no charge separation, while the two other dimers carry unequal charge density between two ET molecules, representing the charge separation $\Delta_n = n_1 - n_2$. The charge separation results in a dipole moment on each of these dimers. Such a charge distribution results in a larger overlap between charge-rich molecules, bonding the related spins (green arrows) into a spin singlet pair that is depicted by a thick green line. This state is not entirely static, but is characterized by an average lifetime τ_{decay}, related to the timescale in Eqs. (10) and (11). Raman active phonons modulate distances between ET molecules resulting in fluctuations of t and J. These fluctuations can lead to the redistribution of charge on $(ET)_2^{1+}$ dimer lattice sites and breaking of spin singlet pairs. We depict that, in the second snapshot [Fig. 6(d)], a Raman active phonon with frequency ω_{ph} that is coupled to the local polarizability interacts with the charge distribution on the $(ET)_2^{1+}$ dimers, breaking the spin singlet pair. In the final state [snapshot Fig. 6(e)], the charge distribution is changed from the initial state [snapshot Fig. 6(c)]: the left and top dimers host electric dipoles which bond their respective spins into a spin single pair, while the right dimer has a charge distribution that is equal between the ET molecules and has one unpaired $S = 1/2$ spin. This scheme demonstrates that, as unpaired spins scatter and dipole moments fluctuate, spin singlets are broken and reformed.

The suggested mechanism implies that antiferromagnetic interactions are involved in the process of dipole-spin-singlet formations and thus phonons are scattered by slow and incoherent spin singlet fluctuations.

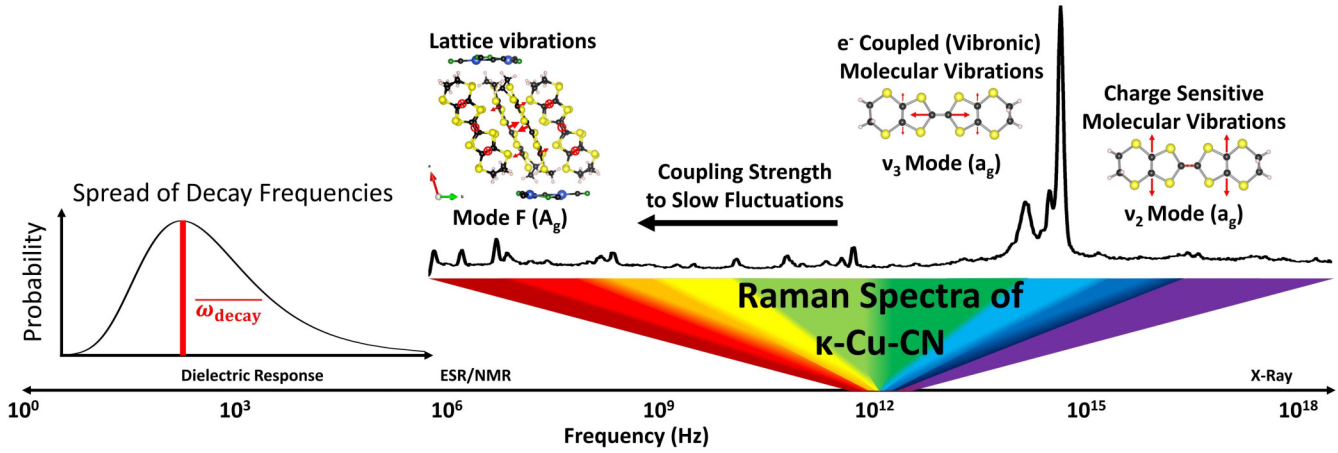

FIG. 7. Scheme summarizing the frequency range of methods used to probe electrodynamic and magnetic response of κ-$(ET)_2Cu_2(CN)_3$. Charge fluctuations have a broad distribution of frequencies ω_{decay}, with the higher parts of the distribution reaching the frequencies of lattice vibrations. The decay process couples more weakly to molecular vibrations, which have frequencies that are an order of magnitude larger than lattice phonons.

C. Experimental sensitivity to fluctuations

The extreme broadening of low frequency modes as temperature approaches 6 K (see Figs. 3 and 4) suggests the stronger electron-phonon coupling term $\frac{\delta\omega_i}{\delta t}$ for these modes and the importance of this term at low frequencies. The increase of Δt is in agreement with the increase of Δn, the amplitude of charge disproportionation, probed by the ν_2 mode below approximately 20 K (see Fig. 2). We have to keep in mind that if fluctuation frequency is small enough ($\omega_{decay} \ll \omega_{phonons}$) we would not be able to distinguish it from a fully static case.

The coupling of phonons to charge fluctuations as discussed above is observed only in the (c,c) scattering channel. Such anisotropy suggests anisotropic charge fluctuations. The anisotropy detected by us is in agreement with the stronger dielectric response with $E \parallel c$ [9] and enhanced optical conductivity, where an additional electronic response that is strongly coupled to lattice phonons increases on cooling below approximately 20 K in the $E \parallel c$ polarization [23,48]. While the authors of Ref. [23] have left the interpretation of the low frequency continuum open, the best candidates for these excitations are charge order fluctuations.

Previously, strong anisotropy of the electronic structure was observed only in the charge ordered state of κ-$(ET)_2Hg(SCN)_2Cl$ by infrared and Raman spectroscopies [31,32] and is in agreement with the theoretically demonstrated renormalization of overlap integrals in the charge ordered state [45]. Our results, as well as Refs. [9,23,48], show that in a fluctuating regime charge disproportionation already shows some anisotropy.

Our conclusions are in agreement with the dielectric measurements in Refs. [8,9], which suggest a slowing down of dipole fluctuations on cooling the samples from 60 K. In order to visualize a comparison among a variety of experimental techniques which probe a broad range of frequencies, such as Raman and dielectric measurements, we present a scheme for experimental sensitivity to slow fluctuations in Fig. 7. The mean relaxation time of the dielectric response 10^{-8} s observed at high temperatures decreases down to an average timescale of 10^{-5} s [8,9]. The relaxation time at around 50 K is close to the characteristic time of lattice phonons, 10^{-11} s. However, the low-temperature behavior where $\omega_{decay} \ll \omega_{ph}$ indeed could be indistinguishable from static regime by Raman scattering. In comparison to the results obtained in different frequency ranges (Fig. 7), we have to keep in mind that any relaxation process described by correlation functions is stochastic. Our correlation function, which is determined by an exponential decay, has an average timescale τ_{decay} and standard deviation of decay times $\sigma_\tau = \sqrt{\langle(\tau - \tau_{decay})^2\rangle} = \tau_{decay}$ [49]. The increase of τ_{decay} naturally leads to the increase of σ_τ, which can cover a range of frequencies from dielectric to Raman and optical measurements (see Fig. 7). Additionally, a large distribution of frequencies is a natural consequence of localized defects emerging from disorder. Such broadening of the characteristic time scales, as well as a broad frequency range of the spectroscopic probes applied to the studies of κ-Cu-CN (see Fig. 7), can explain the rich and at times conflicting experimental results for this material. At finite temperatures below 6 K, defects corresponding to structure, dipoles, and spin can exhibit responses that cover a wide range of frequencies, resembling gapless features.

IV. CONCLUSIONS

Our results demonstrate a dynamic and disordered charge degree of freedom, with an average charge separation of $\Delta n = 0.05e$, and incoherent charge fluctuations within $(ET)_2^{1+}$ dimers, with a decay frequency of ω_{decay}. Our experimental data, in agreement with previous work on this compound, suggest an increase of relaxation time of the fluctuations of disordered charge order in κ-Cu-CN at temperatures below 20 K, which can be considered as a glassy state with a finite relaxation time formed by the electric dipole moments within the $(ET)_2^{1+}$ dimers on a triangular lattice. Our results particularly emphasize the importance of the electron-phonon coupling in the formation of this glassy state in κ-Cu-CN.

Some models which describe similar physical effects already exist. Previously an inhomogeneous state with fluctuating dipoles was observed close to the phase transition from the dimer Mott insulator phase to the charge order insulator phase [37,50]. It is suggested that the intrinsic dynamic inhomogeneity of a system can arise from the competition of Coulomb interactions between charges and antiferromagnetic interactions between $S = 1/2$ spins [37,50]. However, we show that, for an understanding of the charge and magnetic state in this material, a model that is used to describe this transition, for example, a Kugel-Khomskii model [51], should include dynamic electron-phonon coupling.

With electric dipoles on $(ET)_2^{1+}$ dimers mapped onto an Ising model [5,39,40], it is useful to relate our experimental data to recent theoretical work on a disordered transverse Ising model. In our case, disorder can be present in both the amplitude and the orientation of Ising-like electric dipoles. It was shown that when bond randomness is introduced to the transverse Ising model, it can stabilize a structural-spin-glass state [52,53]. This is consistent with our experimental results of disordered electric dipoles with strong coupling to the lattice in κ-Cu-CN. The model has been already successfully applied to different experimental systems, the pyrochlore molybdates, a group of Ising systems, where the Jahn-Teller effect is expected to drive glassy dynamics [54]. These experimental systems carry similarity to κ-Cu-CN, for example in cooling rate effects [10]. Such so called "quantum-mechanically driven structural-spin-glass" exhibits nontrivial thermodynamics, such as a Berezinskii-Kosterlitz-Thouless transition [52], which can be further studied in κ-Cu-CN.

It is important to note that our observation of anisotropic broadening of lattice phonons is so far unique for κ-Cu-CN among molecular Mott insulators, despite observations of charge fluctuations in other systems [11,33,50]. This could be a consequence of differences in the electronic parameters and anisotropy, which leads to the small charge separation Δn observed in κ-Cu-CN. Magnetic exchange Raman scattering observed in the spectra of κ-Cu-CN [11,13,33] shows that, despite finite Δn, the system still behaves as the $S = 1/2$ Mott insulator (dimer Mott insulator) on a triangular lattice, in contrast to other organic Mott insulators with charge fluctuations and charge order [11,37,55].

In summary, we used Raman spectroscopy to probe the electronic state and lattice dynamics of κ-Cu-CN. We observe the development of slowly fluctuating charge disproportionation at temperatures below 60 K. Upon a further decrease in temperature, the charge disproportionation increases in amplitude and the fluctuations slow down. We observe a strong and highly anisotropic coupling of these charge fluctuations to the lattice. Our observations are in agreement with a large number of measurements of the electrodynamic response of κ-Cu-CN, which probed some manifestations of this complex effect. We review theoretical work which shows that this coupling of dipole fluctuations to the lattice can lead to a formation of glassy state. Since dipole fluctuations dynamically renormalize magnetic interactions, our observation suggests the understanding of magnetic properties of κ-Cu-CN as slowly fluctuating spin dimers, reminiscent of the RVB state.

ACKNOWLEDGMENTS

The authors are grateful to C. Hotta and S. Winter for fruitful discussions. The work at JHU was supported by NSF Award No. DMR-2004074. This work was performed in part at Aspen Center for Physics, which is supported by NSF Grant No. PHY-2210452.

[1] P. Anderson, Resonating valence bonds: A new kind of insulator? Mater. Res. Bull. **8**, 153 (1973).

[2] D. A. Huse and V. Elser, Simple variational wave functions for two-dimensional Heisenberg spin-½ antiferromagnets, Phys. Rev. Lett. **60**, 2531 (1988).

[3] G. Misguich, C. Lhuillier, B. Bernu, and C. Waldtmann, Spin-liquid phase of the multiple-spin exchange Hamiltonian on the triangular lattice, Phys. Rev. B **60**, 1064 (1999).

[4] Z. Zhu and S. R. White, Spin liquid phase of the $s = \frac{1}{2}$ $J_1 - J_2$ Heisenberg model on the triangular lattice, Phys. Rev. B **92**, 041105(R) (2015).

[5] C. Hotta, Quantum electric dipoles in spin-liquid dimer Mott insulator κ-$ET_2Cu_2(CN)_3$, Phys. Rev. B **82**, 241104(R) (2010).

[6] BEDT-TTF refers to bis(ethylenedithio)tetrathiafuvalene.

[7] M. Holt, B. J. Powell, and J. Merino, Spin-liquid phase due to competing classical orders in the semiclassical theory of the Heisenberg model with ring exchange on an anisotropic triangular lattice, Phys. Rev. B **89**, 174415 (2014).

[8] M. Abdel-Jawad, I. Terasaki, T. Sasaki, N. Yoneyama, N. Kobayashi, Y. Uesu, and C. Hotta, Anomalous dielectric response in the dimer Mott insulator $\kappa - (BEDT\text{-}TTF)_2Cu_2(CN)_3$, Phys. Rev. B **82**, 125119 (2010).

[9] M. Pinterić *et al.*, Anisotropic charge dynamics in the quantum spin-liquid candidate $\kappa-(BEDT\text{-}TTF)_2Cu_2(CN)_3$, Phys. Rev. B **90**, 195139 (2014).

[10] K. Yakushi, K. Yamamoto, T. Yamamoto, Y. Saito, and A. Kawamoto, Raman spectroscopy study of charge fluctuation in the spin-liquid candidate $\kappa - (BEDT\text{-}TTF)_2Cu_2(CN)_3$, J. Phys. Soc. Jpn. **84**, 084711 (2015).

[11] N. Hassan *et al.*, Evidence for a quantum dipole liquid state in an organic quasi-two-dimensional material, Science **360**, 1101 (2018).

[12] Y. Shimizu, K. Miyagawa, K. Kanoda, M. Maesato, and G. Saito, Spin liquid state in an organic Mott insulator with a triangular lattice, Phys. Rev. Lett. **91**, 107001 (2003).

[13] Y. Nakamura *et al.*, Magnetic Raman scattering study of spin frustrated systems, $\kappa - (BEDT\text{-}TTF)_2X$, J. Phys. Soc. Jpn. **83**, 074708 (2014).

[14] S. Yamashita *et al.*, Thermodynamic properties of a spin-1/2 spin-liquid state in a κ-type organic salt, Nat. Phys. **4**, 459 (2008).

[15] M. Yamashita *et al.*, Thermal-transport measurements in a quantum spin-liquid state of the frustrated triangular magnet κ-$(BEDT\text{-}TTF)_2Cu_2(CN)_3$, Nat. Phys. **5**, 44 (2009).

[16] Y. Shimizu, K. Miyagawa, K. Kanoda, M. Maesato, and G. Saito, Emergence of inhomogeneous moments from spin liquid in the triangular-lattice Mott insulator κ-$(ET)_2Cu_2(CN)_3$, Phys. Rev. B **73**, 140407(R) (2006).

[17] B. Miksch *et al.*, Gapped magnetic ground state in quantum spin liquid candidate κ − BEDT-$TTF_2Cu_2(CN)_3$, Science **372**, 276 (2021).

[18] K. Riedl, R. Valentí, and S. M. Winter, Critical spin liquid versus valence-bond glass in a triangular-lattice organic antiferromagnet, Nat. Commun. **10**, 2561 (2019).

[19] A. Pustogow, T. Le, H. H. Wang, Y. Luo, E. Gati, H. Schubert, M. Lang, and S. E. Brown, Impurity moments conceal low-energy relaxation of quantum spin liquids, Phys. Rev. B **101**, 140401(R) (2020).

[20] R. S. Manna, M. de Souza, A. Brühl, J. A. Schlueter, and M. Lang, Lattice effects and entropy release at the low-temperature phase transition in the spin-liquid candidate κ − $(BEDT\text{-}TTF)_2Cu_2(CN)_3$, Phys. Rev. Lett. **104**, 016403 (2010).

[21] S. Elsässer, D. Wu, M. Dressel, and J. A. Schlueter, Power-law dependence of the optical conductivity observed in the quantum spin-liquid compound κ − $(BEDT\text{-}TTF)_2Cu_2(CN)_3$, Phys. Rev. B **86**, 155150 (2012).

[22] K. Sedlmeier, S. Elsasser, D. Neubauer, R. Beyer, D. Wu, T. Ivek, S. Tomic, J. A. Schlueter, and M. Dressel, Absence of charge order in the dimerized κ-phase BEDT-TTF salts, Phys. Rev. B **86**, 245103 (2012).

[23] M. Dressel, P. Lazic, A. Pustogow, E. Zhukova, B. Gorshunov, J. A. Schlueter, O. Milat, B. Gumhalter, and S. Tomic, Lattice vibrations of the charge-transfer salt κ − $(BEDT\text{-}TTF)_2Cu_2(CN)_3$: Comprehensive explanation of the electrodynamic response in a spin-liquid compound, Phys. Rev. B **93**, 081201(R) (2016).

[24] M. Matsuura, T. Sasaki, M. Naka, J. Muller, O. Stockert, A. Piovano, N. Yoneyama, and M. Lang, Phonon renormalization effects accompanying the 6 k anomaly in the quantum spin liquid candidate κ-$(BEDT\text{-}TTF)_2Cu_2(CN)_3$, Phys. Rev. Res. **4**, L042047 (2022).

[25] See Supplemental Material at http://link.aps.org/supplemental/10.1103/PhysRevB.110.165105 for a detailed description of the fitting procedure, statistical analysis of the charge order and charge glass models, fits of data for a variety of temperatures and polarizations, and mode assignment.

[26] T. Yamamoto *et al.*, Examination of the charge-sensitive vibrational modes in bis (ethylenedithio) tetrathiafulvalene, J. Phys. Chem. B **109**, 15226 (2005).

[27] R. Kubo, A stochastic theory of line shape, Adv. Chem. Phys. **15**, 101 (1969).

[28] J. Sue, Y. J. Yan, and S. Mukamel, Raman excitation profiles of polyatomic molecules in condensed phases. A stochastic theory, J. Chem. Phys. **85**, 462 (1986).

[29] K. Yakushi, Infrared and Raman studies of charge ordering in organic conductors, BEDT-TTF salts with quarter-filled bands, Crystals **2**, 1291 (2012).

[30] B. Efron and R. Tibshirani, *An Introduction to the Bootstrap*, 1st ed. (Chapman and Hall/CRC, New York, 1994), Chap. 12.

[31] N. Drichko, R. Beyer, E. Rose, M. Dressel, J. A. Schlueter, S. A. Turunova, E. I. Zhilyaeva, and R. N. Lyubovskaya, Metallic state and charge-order metal-insulator transition in the quasi-two-dimensional conductor κ-$(BEDT\text{-}TTF)_2Hg(SCN)_2Cl$, Phys. Rev. B **89**, 075133 (2014).

[32] N. M. Hassan, K. Thirunavukkuarasu, Z. Lu, D. Smirnov, E. I. Zhilyaeva, S. Torunova, R. N. Lyubovskaya, and N. Drichko, Melting of charge order in the low-temperature state of an electronic ferroelectric-like system, npj Quantum Mater. **5**, 15 (2020).

[33] N. Hassan *et al.*, Raman scattering as a probe of the magnetic state of BEDT-TTF based Mott insulators, Crystals **8**, 233 (2018).

[34] P. G. Klemens, Anharmonic decay of optical phonons, Phys. Rev. **148**, 845 (1966).

[35] B. E. Vugmeister and M. D. Glinchuk, Dipole glass and ferroelectricity in random-site electric dipole systems, Rev. Mod. Phys. **62**, 993 (1990).

[36] Y. Nakamura *et al.*, Anion arrangement effects on electronic states of κ-type BEDT-TTF compounds, J. Phys. Soc. Jpn. **90**, 054703 (2021).

[37] M. Yamashita *et al.*, Ferromagnetism out of charge fluctuation of strongly correlated electrons in κ-$(BEDTTTF)_2Hg(SCN)_2Br$, npj Quantum Mater. **6**, 87 (2021).

[38] S. Dayal, R. T. Clay, H. Li, and S. Mazumdar, Paired electron crystal: Order from frustration in the quarter-filled band, Phys. Rev. B **83**, 245106 (2011).

[39] M. Naka and S. Ishihara, Electronic ferroelectricity in a dimer Mott insulator, J. Phys. Soc. Jpn. **79**, 063707 (2010).

[40] M. Naka and S. Ishihara, Collective charge excitation in a dimer Mott insulating system, J. Phys. Soc. Jpn. **82**, 023701 (2013).

[41] K. Nakamura, Y. Yoshimoto, T. Kosugi, R. Arita, and M. Imada, *Ab initio* derivation of low-energy model for κ-ET type organic conductors, J. Phys. Soc. Jpn. **78**, 083710 (2009).

[42] H. C. Kandpal, I. Opahle, Y.-Z. Zhang, H. O. Jeschke, and R. Valentí, Revision of model parameters for κ-type charge transfer salts: An *ab initio* study, Phys. Rev. Lett. **103**, 067004 (2009).

[43] H. O. Jeschke, M. de Souza, R. Valenti, R. S. Manna, M. Lang, and J. A. Schlueter, Temperature dependence of structural and electronic properties of the spin-liquid candidate κ-$(BEDT\text{-}TTF)_2Cu_2(CN)_3$, Phys. Rev. B **85**, 035125 (2012).

[44] T. Koretsune and C. Hotta, Evaluating model parameters of the κ- and β'-type Mott insulating organic solids, Phys. Rev. B **89**, 045102 (2014).

[45] A. C. Jacko, E. P. Kenny, and B. J. Powell, Interplay of dipoles and spins in $\kappa - (BEDT - TTF)_2X$, where $X = Hg(SCN)_2Cl$, $Hg(SCN)_2Br$, $Cu[N(CN)_2]Cl$, $Cu[N(CN)_2]Br$, and $Ag_2(CN)_3$, Phys. Rev. B **101**, 125110 (2020).

[46] H. Mori *et al.*, The intermolecular interaction of tetrathiafulvalene and bis(ethylenedithio)tetrathiafulvalene in organic metals. calculation of orbital overlaps and models of energy-band structures, Bull. Chem. Soc. Jpn. **57**, 627 (1984).

[47] T. Isono, T. Terashima, K. Miyagawa, K. Kanoda, and S. Uji, Quantum criticality in an organic spin-liquid insulator κ-$(BEDT\text{-}TTF)_2Cu_2(CN)_3$, Nat. Commun. **7**, 13494 (2016).

[48] K. Itoh, H. Itoh, M. Naka, S. Saito, I. Hosako, N. Yoneyama, S. Ishihara, T. Sasaki, and S. Iwai, Collective excitation of an electric dipole on a molecular dimer in an organic dimer-Mott insulator, Phys. Rev. Lett. **110**, 106401 (2013).

[49] J. Kingman, *Poisson Processes*, Oxford Studies in Probability (Clarendon Press, Oxford, 1992).

[50] M. Urai *et al.*, Anomalously field-susceptible spin clusters emerging in the electric-dipole liquid candidate κ-$(ET)_2Hg(SCN)_2Br$, Sci. Adv. **8**, eabn1680 (2022).

[51] K. I. Kugel' and D. I. Khomskĭ, The Jahn-Teller effect and magnetism: transition metal compounds, Sov. Phys. Usp. **25**, 231 (1982).

[52] C. Hotta, K. Ueda, and M. Imada, Quantum mechanically driven structural-spin glass in two dimensions at finite temperature, arXiv:2207.07293.

[53] C. Hotta, T. Yoshida, and K. Harada, Quantum critical dynamics in the two-dimensional transverse Ising model, Phys. Rev. Res. **5**, 013186 (2023).

[54] K. Mitsumoto, C. Hotta, and H. Yoshino, Supercooled Jahn-Teller ice, Phys. Rev. Res. **4**, 033157 (2022).

[55] N. Drichko *et al.*, Charge and spin interplay in a molecular-dimer-based organic Mott insulator, Phys. Rev. B **106**, 064202 (2022).